

Electromagnetic modeling of induced polarization with the fictitious wave domain method

Rune Mittet, EMGS

SUMMARY

The fictitious wave domain method makes a numerically effective implementation of finite-difference simulations of low-frequency electromagnetic field propagation in the earth feasible. Up until now frequency dependent conductivity has not been considered with this method. Thus, modeling of induced polarization (IP) effects has not been possible with the fictitious wave domain method. IP effects can be modeled with this method if a modified Debye medium is introduced. The frequency dependent conductivity spectrum due to the modified Debye medium must be fitted to the desired conductivity spectrum in the same way as the Cole-Cole distribution is fitted to the desired conductivity spectrum.

INTRODUCTION

It is well established that purely diffusive systems can be modeled in a fictitious wave domain followed by a temporal transform that can either give results in the diffusive time domain or the diffusive frequency domain (Lee et al. , 1989; de Hoop, 1996; Mittet, 2010). One main reason for choosing this strategy is a significant reduction in computer time for modeling low frequency electromagnetic field propagation in the earth (Maaø, 2007; Mittet , 2010).

Up until now frequency-dependent conductivity has not been considered with this method. Thus, modeling of induced polarization (IP) effects has not been possible with the fictitious wave domain method. In particular, modeling of IP effects is important when prospecting for metallic ore bodies but sedimentary rocks above hydrocarbon reservoirs may also be influenced by IP effects due to the formation of for example pyrite.

Frequency-dependent conductivity results in principle in a convolution between the conductivity and the electric field in the time domain. Straightforward implementation of the IP effect as a temporal convolution is numerically costly in modeling since the time history of the conductivity must be stored. The corresponding problem in seismic modeling leads to a convolution of the bulk modulus with the strain. The numerical implementation problem was here solved with the introduction of memory functions (Emmerich and Korn, 1987). Emmerich and Korn (1987) used the Standard Linear Solid (SLS) rheological models as analogs for the medium behavior. Mittet and Renli (1996) discussed an elastic finite-difference implementation with anisotropy and absorption giving calibration examples with other numerical schemes and how this method could give simulation results that matched real data.

An electromagnetic analog handling anisotropy and IP effects is developed here. Dispersive propagation in non-conducting media is discussed in Taflove and Hagness (2005). The Debye medium discussed there is similar to the SLS in acoustics or

elastics. The resulting modeling-domain medium will not be a true Debye medium for the implementation discussed here. This is due to the transform from the fictitious wave domain to the diffusive domain. However, the resulting medium will have similarities to a Debye medium so it is here named a modified Debye medium.

THEORY

We shall here be concerned with electromagnetic field propagation. The electromagnetic fields will be analyzed in both the time and the frequency domain. The following Fourier transform convention is used,

$$\Psi(\omega) = \int_{-\infty}^{\infty} dt \Psi(t) e^{i\omega t}, \quad (1)$$

with opposite sign in the exponent for the inverse transform. Here ω is real. We will also need the transform that takes the fields from the fictitious time domain to the “real-world” frequency domain (Mittet, 2010). Let ω' be a complex angular frequency with a positive imaginary part, $\omega' = \Re(\omega') + i\Im(\omega')$. Assume that the field Ψ is strictly causal such that $\Psi(t=0) = 0.0$, $\partial_t \Psi(t=0) = 0.0$. and that the final time, T , of the transform,

$$\Psi(\omega') = \int_0^T dt \Psi(t) e^{i\omega' t}, \quad (2)$$

is sufficiently large such that,

$$\Psi(T) e^{-\Im(\omega')T} \approx 0.0, \quad (3)$$

which is fulfilled if the field, Ψ , has died out at the final time or if the product of the imaginary part of ω' and the final time is sufficiently large. With the above conditions we find,

$$\begin{aligned} \int_0^T dt \partial_t \Psi(t) e^{i\omega' t} &= -i\omega' \Psi(\omega'), \\ \int_0^T dt \partial_t^2 \Psi(t) e^{i\omega' t} &= -\omega'^2 \Psi(\omega'), \end{aligned} \quad (4)$$

with $\Psi(\omega')$ given by equation 2.

Electromagnetic case without IP effects

The main elements of the fictitious wave domain method for electromagnetic fields is given in Mittet (2010). The conductivity is assumed independent of frequency in this case. The anisotropic non-diffusive representation of the Maxwell equations is,

$$\begin{aligned} -\nabla \times \mathbf{H}'(\mathbf{x}, t') + \boldsymbol{\varepsilon}'(\mathbf{x}) \partial_{t'} \mathbf{E}'(\mathbf{x}, t') &= -\mathbf{J}'(\mathbf{x}, t'), \\ \nabla \times \mathbf{E}'(\mathbf{x}, t') + \mu \partial_{t'} \mathbf{H}'(\mathbf{x}, t') &= 0, \end{aligned} \quad (5)$$

where $\boldsymbol{\varepsilon}'(\mathbf{x})$ is the electric permittivity tensor. The magnetic permeability μ is assumed isotropic and equal to the value in vacuum. \mathbf{E}' and \mathbf{H}' are electric and magnetic vector fields. The

IP with fictitious time domain method

source term is the electric current density, \mathbf{J}' . The primes for the electric fields, the magnetic fields and the electric permittivity tensor in equation 5 are used to distinguish these fictitious wave domain fields from the observable fields which will be without primes.

Applying the transform in equation 2 on two Maxwell equations give,

$$\begin{aligned} -\nabla \times \mathbf{H}'(\mathbf{x}, \omega') - i\omega' \boldsymbol{\epsilon}'(\mathbf{x}) \mathbf{E}'(\mathbf{x}, \omega') &= -\mathbf{J}'(\mathbf{x}, \omega'), \\ \nabla \times \mathbf{E}'(\mathbf{x}, \omega') - i\omega' \mu \mathbf{H}'(\mathbf{x}, \omega') &= 0. \end{aligned} \quad (6)$$

At this stage I make a particular choice for the complex angular frequency,

$$\omega' = \sqrt{2i\omega_0\omega}, \quad (7)$$

where ω is a real angular frequency and ω_0 is a real positive scale parameter. Ampère's law in equation 6 is multiplied with the ratio ω'/ω to give,

$$\begin{aligned} -\nabla \times \left(\frac{\omega'}{\omega} \mathbf{H}'(\mathbf{x}, \omega') \right) - i \frac{\omega'^2}{\omega} \boldsymbol{\epsilon}'(\mathbf{x}) \mathbf{E}'(\mathbf{x}, \omega') &= -\frac{\omega'}{\omega} \mathbf{J}'(\mathbf{x}, \omega'), \\ \nabla \times \mathbf{E}'(\mathbf{x}, \omega') - i\omega\mu \left(\frac{\omega'}{\omega} \mathbf{H}'(\mathbf{x}, \omega') \right) &= 0. \end{aligned} \quad (8)$$

Equations for observable fields, \mathbf{E} and \mathbf{H} , are then obtained by the substitutions,

$$\begin{aligned} \boldsymbol{\epsilon}'(\mathbf{x}) &= \frac{\boldsymbol{\sigma}(\mathbf{x})}{2\omega_0} \\ -i \frac{\omega'^2}{\omega} \boldsymbol{\epsilon}'(\mathbf{x}) &= \boldsymbol{\sigma}(\mathbf{x}) \\ \mathbf{E}'(\mathbf{x}, \omega) &= \mathbf{E}'(\mathbf{x}, \omega') \\ \mathbf{H}(\mathbf{x}, \omega) &= \frac{\omega'}{\omega} \mathbf{H}'(\mathbf{x}, \omega') = \sqrt{\frac{2\omega_0}{-i\omega}} \mathbf{H}'(\mathbf{x}, \omega') \\ \mathbf{J}(\mathbf{x}, \omega) &= \frac{\omega'}{\omega} \mathbf{J}'(\mathbf{x}, \omega') = \sqrt{\frac{2\omega_0}{-i\omega}} \mathbf{J}'(\mathbf{x}, \omega') \end{aligned} \quad (9)$$

where $\boldsymbol{\sigma}$ is the conductivity tensor. Equations 8 are by these substitutions equal to the Maxwell equations in the quasi-static limit,

$$\begin{aligned} -\nabla \times \mathbf{H}(\mathbf{x}, \omega) + \boldsymbol{\sigma}(\mathbf{x}) \mathbf{E}(\mathbf{x}, \omega) &= -\mathbf{J}(\mathbf{x}, \omega), \\ \nabla \times \mathbf{E}(\mathbf{x}, \omega) - i\omega\mu \mathbf{H}(\mathbf{x}, \omega) &= 0. \end{aligned} \quad (10)$$

The modeling approach is to solve equations 5 by finite differences. The time domain fields are transformed to the frequency domain by equation 2 with the particular complex angular frequency given in equation 7. The source scaling is explained in Mittet (2010) with more considerations in Mittet (2015).

Electromagnetic case with IP effects

The implementation of absorption in time domain seismic or borehole modeling is commonly performed by introducing additional equations that have a rheological analog in terms of springs and dashpots (Emmerich and Korn, 1987). Thus, a set of first-order differential equations are added to the system of Newton's second law and Hooke's law. The added differential equations are for auxiliary fields that are commonly

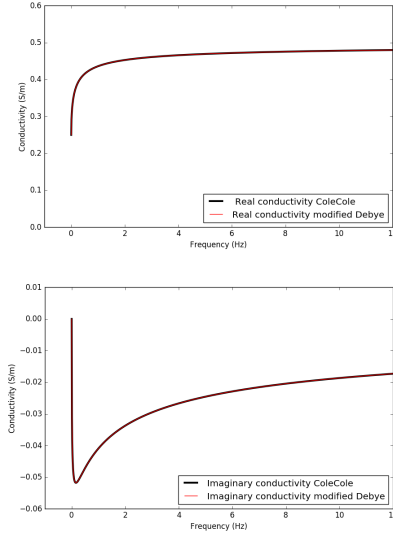


Figure 1: Real and imaginary part of conductivity spectra. Black curves for the Cole-Cole medium and red curves for the modified Debye medium.

referred to as memory variables. I will introduce a similar system here. Instead of springs and dashpots the analogs should now in principle be electric in nature. However, such analogs are used for illustration only and are actually not needed. The consequences of adding the first-order differential equations to the system must of course be analyzed and understood. Good analogs are hard to find for the method discussed here since the absorption and dispersion properties will be anomalous in the fictitious wave domain where the medium will be effectual, not absorbing, and the low-frequency propagation velocity will be higher than the high-frequency propagation velocity which is contrary to normal dispersion. There is a slight boosting of amplitudes with propagated distance in the fictitious wave domain when IP effects are added. This effect has not caused runaway solutions in practical modeling examples up to now but does represent a potential problematic issue in the case of long modeling times.

The equation system to solve is,

$$\begin{aligned} -\nabla \times \mathbf{H}'(\mathbf{x}, t') + \boldsymbol{\epsilon}'^{\infty}(\mathbf{x}) \partial_{t'} \mathbf{E}'(\mathbf{x}, t') - \\ \sum_{v=1}^M \mathbf{U}^v(\mathbf{x}, t') = -\mathbf{J}'(\mathbf{x}, t'), \\ \nabla \times \mathbf{E}'(\mathbf{x}, t') + \mu \partial_{t'} \mathbf{H}'(\mathbf{x}, t') = 0, \\ \partial_{t'} \mathbf{U}^v(\mathbf{x}, t') + \omega^v \mathbf{U}^v(\mathbf{x}, t') = \omega^v \Delta \boldsymbol{\epsilon}'^{IV}(\mathbf{x}) \partial_{t'} \mathbf{E}'(\mathbf{x}, t'), \end{aligned} \quad (11)$$

where ω^v is a resonance frequency and \mathbf{U}^v is the memory variable vector field. There is one first-order partial differential equation added for each resonance mechanism. In total there

IP with fictitious time domain method

are M resonances. Let,

$$\Delta\boldsymbol{\epsilon}'(\mathbf{x}) = \sum_{v=1}^M \Delta\boldsymbol{\epsilon}'^v(\mathbf{x}). \quad (12)$$

The low-frequency limit for the electric permittivity tensor,

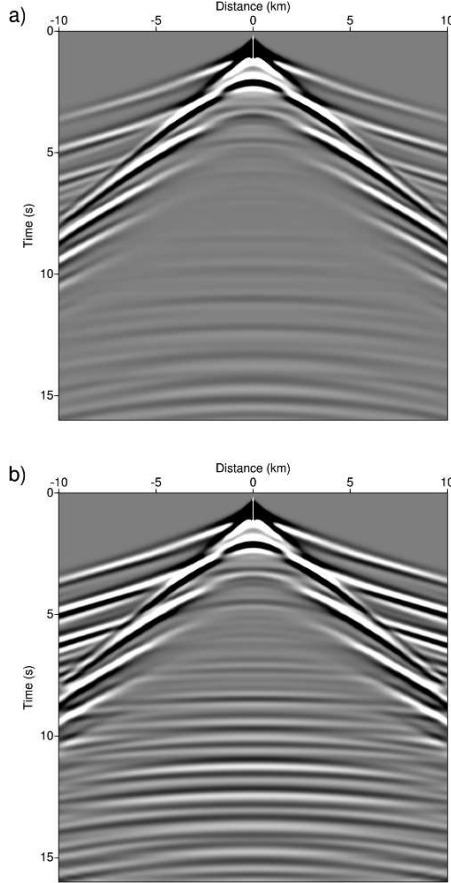


Figure 2: Shotgathers for inline electric fields from fictitious wave domain modeling. The bottom gather is for a simulation where IP effects were included. The anomalous behavior with increased amplitude with propagation distance/time is clearly visible.

$\boldsymbol{\epsilon}'^0$, and the high-frequency limit for the electric permittivity tensor, $\boldsymbol{\epsilon}'^\infty$, are then related as $\boldsymbol{\epsilon}'^\infty(\mathbf{x}) = \boldsymbol{\epsilon}'^0(\mathbf{x}) + \Delta\boldsymbol{\epsilon}'(\mathbf{x})$. A standard Fourier transform with a real angular frequency, ω , gives for the memory variables in equation 11,

$$\mathbf{U}^v(\mathbf{x}, \omega) = \frac{-i\omega\omega^v\Delta\boldsymbol{\epsilon}'^v(\mathbf{x})\mathbf{E}'(\mathbf{x}, \omega)}{\omega^v - i\omega} \quad (13)$$

Ampère's law in equation 11 can, in the frequency domain, be written as,

$$-\nabla \times \mathbf{H}'(\mathbf{x}, \omega) - i\omega\boldsymbol{\epsilon}'(\mathbf{x}, \omega)\mathbf{E}'(\mathbf{x}, \omega) = -\mathbf{J}'(\mathbf{x}, \omega), \quad (14)$$

with

$$\boldsymbol{\epsilon}'(\mathbf{x}, \omega) = \boldsymbol{\epsilon}'^\infty(\mathbf{x}) - \sum_{v=1}^M \frac{\omega^v\Delta\boldsymbol{\epsilon}'^v(\mathbf{x})}{\omega^v - i\omega}. \quad (15)$$

It is now obvious that the introduction of the set of first order partial differential equations leads to an electric permittivity tensor that is frequency dependent. We see that dielectric permittivity depends on a sum of Debye relaxation mechanisms. In some cases it may be sufficient to include only one mechanism, $M = 1$, if necessary more resonances can be included. The parameters in equation 15 can be optimized such that $\boldsymbol{\epsilon}'(\mathbf{x}, \omega)$ is close to an observed spectrum for a given frequency band.

The above system is well known for a frequency dependent electric permittivity in a polarizing medium. The auxiliary memory field in equation 11 has the time-domain solution,

$$\mathbf{U}^v(\mathbf{x}, t') = e^{-\omega^v t'} \int_0^{t'} dt'' \omega^v \Delta\boldsymbol{\epsilon}'^v(\mathbf{x}) [\partial_{t''} \mathbf{E}'(\mathbf{x}, t'')] e^{\omega^v t''}. \quad (16)$$

Equation 16 can be solved by time stepping. Assume the simulation time step is Δt . Further on, let $t^n = n\Delta t$ and the forward staggered timestep be $t^N = (n + \frac{1}{2})\Delta t$, then,

$$\mathbf{U}^v(\mathbf{x}, t^{n+1}) = \mathbf{U}^v(\mathbf{x}, t^n) e^{-\omega^v \Delta t} + \Delta\boldsymbol{\epsilon}'^v(\mathbf{x}) \dot{\mathbf{E}}'(\mathbf{x}, t^N) (1 - e^{-\omega^v \Delta t}). \quad (17)$$

Equation 17 serves to demonstrate that $\mathbf{U}^v(\mathbf{x}, t^{n+1})$ can be calculated based on previous time steps. The actual implementation is slightly more complicated to achieve maximum accuracy.

The immediate problem is that our formulation is for waves in the fictitious time domain. We need a formulation for diffusive low frequency geo-electric fields. Equation 11 can be transformed with the complex frequency, $\sqrt{2i\omega_0\omega}$, to obtain,

$$\begin{aligned} -\nabla \times \mathbf{H}(\mathbf{x}, \omega) + \boldsymbol{\sigma}(\mathbf{x}, \omega)\mathbf{E}(\mathbf{x}, \omega) &= -\mathbf{J}(\mathbf{x}, \omega), \\ \nabla \times \mathbf{E}(\mathbf{x}, \omega) - i\omega\boldsymbol{\mu}\mathbf{H}(\mathbf{x}, \omega) &= 0, \end{aligned} \quad (18)$$

with,

$$\boldsymbol{\sigma}(\mathbf{x}, \omega) = \boldsymbol{\sigma}^\infty(\mathbf{x}) - \sum_{v=1}^N \frac{\omega^v \Delta\boldsymbol{\sigma}^v(\mathbf{x})}{\omega^v + \sqrt{\omega_0\omega} - i\sqrt{\omega_0\omega}}. \quad (19)$$

The diffusive system given by equations 18 and 19 does not describe a Debye medium since the angular frequency is under the square root. However, if the spectrum in equation 19 can be fitted to an IP spectrum then modeling of low-frequency geo-electric fields with IP effects included, using the fictitious time domain method is feasible. In principle this is similar to representing the conductivity spectrum with a Cole-Cole model (Cole and Cole, 1941).

If $\boldsymbol{\sigma}^\infty$, $\Delta\boldsymbol{\sigma}^v$ and ω^v are estimated, then the electric permittivities needed for the fictitious wave domain simulation are given by,

$$\begin{aligned} \boldsymbol{\epsilon}'^\infty(\mathbf{x}) &= \frac{\boldsymbol{\sigma}^\infty(\mathbf{x})}{2\omega_0}, \\ \Delta\boldsymbol{\epsilon}'^v(\mathbf{x}) &= \frac{\Delta\boldsymbol{\sigma}^v(\mathbf{x})}{2\omega_0}. \end{aligned} \quad (20)$$

IP with fictitious time domain method

RESULTS

For simplicity we assume isotropy and a single resonance mechanism, ($\nu = 1$). A Cole-Cole distribution

$$\sigma(\omega) = \sigma^\infty \left(1 - \frac{\eta}{1 + (-i\omega\tau)^c} \right) \quad (21)$$

is introduced as a reference case. The Cole-Cole distribution has $\sigma^\infty = 0.5$ S/m, a chargeability of $\eta = 0.5$, a time constant $\tau = 1.0$ s and a relaxation constant $c = 0.5$. To simulate a medium with these properties we need to optimize σ^∞ , $\Delta\sigma^1$ and ω^1 in,

$$\sigma(\omega) = \sigma^\infty - \frac{\omega^1 \Delta\sigma^1}{\omega^1 + \sqrt{\omega_0 \omega} - i\sqrt{\omega_0 \omega}}, \quad (22)$$

such that the two spectra are as close as possible. A least square fit gives $\sigma^\infty = 0.5$ S/m as for the Cole-Cole distribution. Further on $\Delta\sigma^1 = 0.25$ S/m and $\omega^1 = 3.008$ Hz. The value for ω_0 is the same as used in Mittet (2015), $\omega_0 = 2\pi f_0$ with $f_0 = 0.7198$ Hz. The fit is in this case excellent for frequencies well above 100 Hz. Curves for the interval 0 to 12 Hz are shown in Figure 1. The Cole-Cole relaxation constant

depends on the square root of angular frequency in the denominator. This makes it easier to fit the two spectra. However, almost equal spectra can also be obtained for relaxation constants different from 0.5. If necessary more than one resonance can be used for the modified Debye model.

A simulation of marine acquisition was performed for a model both with and without a layer having IP effects. The model consists of plane layers which makes it possible to compare the fictitious wave domain method with a direct solution in the frequency domain using a plane layer modeling code as described by Løseth and Ursin (2007). The top halfspace is air. The waterlayer is 1 km thick with conductivity 3.2 S/m. The top formation is 300 m thick with conductivity 1 S/m. The next layer is 1800 m thick with conductivity 0.5 S/m. It is this layer that will also be modeled with the IP effects as described above. The bottom layer is a halfspace with conductivity 0.25 S/m. The fictitious wave domain inline electric fields are shown in Figure 2.

The inline electric fields can be transformed to the frequency domain by the transform in equation 2 using the particular choice in equation 7. The result for 0.20 Hz is shown in Figure 3. The black curves in Figure 3a and 3b are for plane layer modeling and no IP effects in the second formation layer. The red curves are the corresponding fictitious wave domain results. The blue curves in Figure 3a and 3b are for plane layer modeling with IP effects in the second formation layer. The cyan curves are the corresponding fictitious wave domain results. The black curve in Figure 3c is for plane layer modeling and the green curve in Figure 3c is for fictitious wave domain modeling. Both curves measure the amplitude enhancement due of the IP effects by calculating,

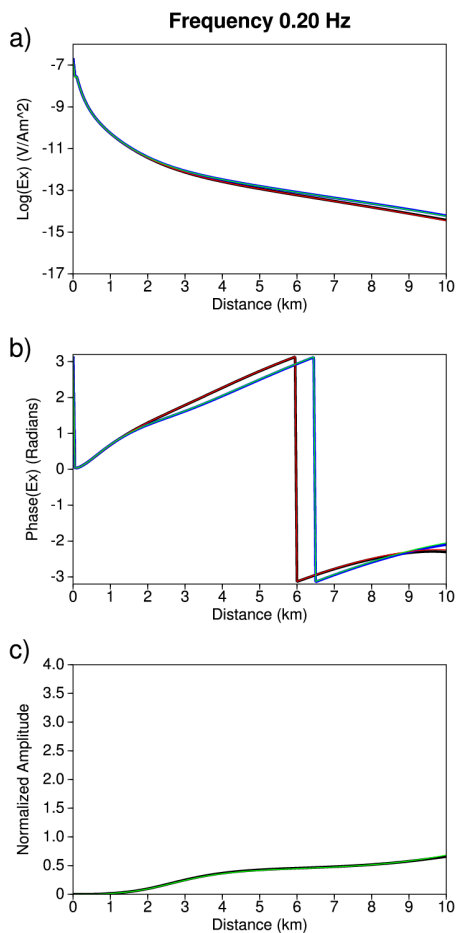


Figure 3: Inline electric fields. a) Amplitudes curves. b) Phase curves c) Normalized amplitudes.

equals 0.5 in this case and the modified Debye medium also

$$R = \frac{|E_x^{IP} - E_x^B|}{|E_x^B|} \quad (23)$$

where E_x^B is field calculated assuming no IP effects. From Figure 3b we observe that the IP effects result in a delay of the signal. This since the slope of the phase curve is smaller when IP effects are included. The fit between the plane layer modeling and the fictitious wave domain modeling is very good for the 0.2 Hz contribution shown here, but also for a much wider frequency range.

CONCLUSIONS

Frequency dependent effects like induced polarization can be modeled with the fictitious wave domain method. The absorption/dispersion laws in the wave domain are anomalous in the sense that field amplitudes are boosted as a function of propagation distance and that the relaxed phase velocity is higher than the unrelaxed phase velocity. However, after transformation to observable fields in the frequency domain we observe excellent correlation with solutions based on a direct solution in the frequency domain.

REFERENCES

- Cole, K. S., and R. H. Cole, 1941, Dispersion and absorption in dielectrics i. alternating current characteristics: *The Journal of chemical physics*, **9**, 341–351.
- de Hoop, A. T., 1996, A general correspondence principle for time-domain electromagnetic wave and diffusion fields: *Geophysical Journal International*, **127**, 757–761.
- Emmerich, H., and M. Korn, 1987, Incorporation of attenuation into time-domain computations of seismic wave fields: *Geophysics*, **52**, 1252–1264, <https://doi.org/10.1190/1.1442386>.
- Lee, K. H., G. Liu, and H. F. Morrison, 1989, A new approach to modeling the electromagnetic response of conductive media: *Geophysics*, **54**, 1180–1192, <https://doi.org/10.1190/1.1442753>.
- Løseth, L., and B. Ursin, 2007, Electromagnetic fields in planarly layered anisotropic media: *Geophysical Journal International*, **170**, 44–80, <https://doi.org/10.1111/j.1365-246X.2007.03390.x>.
- Maaø, F. A., 2007, Fast finite-difference time-domain modeling for marine-subsurface electromagnetic problems: *Geophysics*, **72**, no. 2, A19–A23, <https://doi.org/10.1190/1.2434781>.
- Mittet, R., 2010, High-order finite-difference simulations of marine CSEM surveys using a correspondence principle for wave and diffusion fields: *Geophysics*, **75**, no. 1, F33–F50, <https://doi.org/10.1190/1.3278525>.
- Mittet, R., 2015, Seismic wave propagation concepts applied to the Interpretation of marine controlled-source electromagnetic: *Geophysics*, **80**, no. 2, E63–E81, <https://doi.org/10.1190/geo2014-0215.1>.
- Mittet, R., and L. Renlie, 1996, High-order finite-difference modeling of multipole logging in formations with anisotropic attenuation and elasticity. *Geophysics*, **61**, 21–33, <https://doi.org/10.1190/1.1443942>.
- Taflove, A., and S. C. Hagness, 2005, *Computational electrodynamics: The finite-difference time-domain method*: Artech house.